ЖЭТФ, 2015, том 147, вып. 3, стр. 526–535

TUNNELLING WITH WORMHOLE CREATION

S. Ansoldi [a,b], ***T. Tanaka*** [c,d*]

[a] *National Institute of Nuclear Physics (INFN), I-34149, Trieste, Italy*

[b] *University of Udine, I-33100, Udine, Italy*

[c] *Department of Physics, Kyoto University, 606-8502, Kyoto, Japan*

[d] *Yukawa Institute for Theoretical Physics, Kyoto University, 606-8502, Kyoto, Japan*

Received October 18, 2014

The description of quantum tunnelling in the presence of gravity shows subtleties in some cases. We discuss wormhole production in the context of the spherically symmetric thin-shell approximation. By presenting a fully consistent treatment based on canonical quantization, we solve a controversy present in the literature.

Contribution for the JETP special issue in honor of V. A. Rubakov's 60th birthday

DOI: 10.7868/S0044451015030143

1. INTRODUCTION

Quantum tunnelling plays various roles in cosmology. For instance, false vacuum decay through quantum tunnelling [1–3] is an important process for the universe to visit many vacua in the string landscape [4–6]. Also, the possibility of creation of an open universe through false vacuum decay has been extensively discussed [7–10]. Properly taking the effect of gravity into account can be quite nontrivial. Although the effect of gravity is secondary in some cases, there are in fact several cases where gravity plays a crucial role, such as the upward quantum tunnelling from a lower- to a higher-energy vacuum [11, 12].

Even when the effect of gravity is secondary, including gravity can make the treatment highly nontrivial. One example is the subtle issue raised by Lavrelashvili, Rubakov, and Tinyakov [13] that fluctuations around bubble nucleation might cause an instability, which leads to explosive particle production. One prescription to cure this pathology was proposed in Refs. [14, 15], where it is shown that the instability can be eliminated, at least apparently, by an appropriate choice of the gauge.

Quantum tunnelling in connection with gravity has been discussed also in other contexts. One of them is wormhole formation [16–24], which is the main subject of this paper. Wormhole formation is a signature of what is also referred to in the literature as baby/child universe creation [25]. Spherical thin shells with various equations of state have been studied as models of matter fields able to describe this process. Even in the simple case of a pure tension shell, the quantum mechanical formation of a wormhole seems possible. However, some inconsistencies between different prescriptions seem to exist in the literature [26]. In this paper, we show that the origin of these apparent discrepancies is tightly related to the use of the time coordinate in the static chart. We then propose a plausible prescription based on a smooth time-slicing to tackle the problem.

This paper is organized as follows. In Sec. 2, we briefly review the derivation of the standard result for the tunnelling amplitude based on the direct evaluation of the action, when the time slice of the static chart is used. In Sec. 3, we discuss the problem that arises when we try to apply the conventional formula to situations characterized by wormhole production. To overcome some difficulties that appear in this last case, in Sec. 4 we then study the same problem using the canonical approach with a smooth time slice: this allows us to derive the formula for the tunnelling rate without any ambiguity. In Sec. 5, we finally show how the same formula can be reproduced by the direct evaluation of the action if we carefully take the smooth time slice. Section 6 is devoted to a summary and discussion: we also elaborate on a remaining, more subtle, issue.

*E-mail: tanaka@yukawa.kyoto-u.ac.jp

2. CONVENTIONAL APPROACH

In this paper, we consider the simplest spherically symmetric domain-wall model, whose Lagrangian is given by

$$S = \frac{1}{16\pi G}\int d^4x\sqrt{-g}\,\mathcal{R} - \int d\tau\, m(\hat{R}), \qquad (1)$$

where $\mathcal{R}$ is the scalar curvature and $m(\hat{R})$ is the radius-dependent mass of the wall, e. g., $m(\hat{R}) = \text{const}$ for a dust domain wall, while $m(\hat{R}) = 4\pi\sigma\hat{R}^2$ for a wall consisting of pure tension σ; moreover, τ is the proper time along the wall, and $\hat{R}$ denotes the circumferential radius of the wall. In general, quantities marked with a hat are assumed to be evaluated at the position of the wall, e. g., $\hat{B} = \hat{B}(t) = B(t, \hat{r}(t))$ if B is a function of t and r, and $r = \hat{r}(t)$ is one possible parameterization of the wall trajectory. Depending on the model parameters, the wall motion can have some classically forbidden region for a range of the radius. We are interested in discussing the quantum tunnelling of the wall when it reaches a turning point, i. e., a boundary of the classically forbidden region, by explicitly taking gravity into account.

In this section, we derive a conventional but incorrect formula for the tunnelling rate of the wall. Although we mostly follow Ref. [27], we do not claim that the result obtained there is wrong. Indeed, our emphasis is about the fact that the authors of Ref. [27] clearly identified a discrepancy between the direct evaluation of the action that they propose and a naive canonical approach. Moreover, it was clearly emphasized in Ref. [27] that the proposed direct approach guarantees, instead, a continuous variation of the action as the parameters (the Schwarzschild mass, the de Sitter cosmological constant, the wall surface tension in their model) are changed: on the contrary, the conventional canonical approach does not guarantee the continuity of the action as a function of the parameters. At the same time, the direct calculation of the action reveals difficulties in the identification of the Euclidean manifold interpolating between the before- and after-tunnelling classical solutions in a consistent way: indeed, Farhi et al. associate what they call a *pseudo-manifold* to the instanton solution. The direct approach defines the pseudo-manifold by weighing different volumes of the instanton along the classically forbidden trajectory by an integer number that counts how many times (and in which direction) the Euclidean volume is swept by the time slice. We show in what follows that the canonical approach, in full generality, can reproduce the same value for the tunnelling action given in the approach proposed in [27].

The direct evaluation of the action is possible because the solution is simply given by a junction of two spacetimes. Here, for simplicity, we assume that both the inside and outside of the bubble are empty, and hence the inside can be taken as a piece of Minkowski spacetime and the outside as a piece of Schwarzschild spacetime. (In Ref. [27], the inside was equipped with a vacuum energy density, i. e., a cosmological constant, but this does not change the treatment in any substantial way.) The method proposed in [27] was developed in coordinates adapted to the static and spherically symmetric nature of the spacetimes participating in the junction. With this, we mean that the Lagrangian was preferably considered in connection with the coordinate times in the static chart in both spacetime regions, which we denote by t_{S} and t_{M} in the simplified case that we consider here. However, most of the calculations were performed using the proper time of an observer sitting on the junction, and therefore the result can be easily extended to a coordinate-independent expression, as we see in Sec. 5.

The contributions to the action can be summarized as follows.

1. A matter term coming from the shell, $I^{\mathrm{wall}}_{\mathrm{matter}}$: this is nothing but the contribution from the stress–energy tensor localized on the bubble surface.

2. A gravity term coming from the bubble wall, $I^{\mathrm{wall}}_{\mathrm{gravity}}$: this is, basically, the well-known *extrinsic-curvature-trace-jump* term.

3. The bulk contributions vanish for classical solutions since there is no matter in the bulk.

4. Surface terms: although the appearance of surface terms is conceptually clear, the treatment of these terms may be nontrivial. As clearly discussed in Ref. [27], several contributions arise.

(a) The crucial contribution in [27], $I^{\mathrm{wall}}_{\mathrm{surface}}$, comes from the bubble wall positions, where the normal to the constant-time surface is discontinuous. However, this contribution does not appear if we adopt a smooth foliation of time across the wall. In Sec. 4, we take this last picture.

(b) Another contribution comes from a surface at a large constant circumferential radius in the outside spacetime, $I^{R_{\mathrm{BIG}}}_{\mathrm{surface}}$: this cut-off radius allows us to work with a (spatially) bounded volume, and the large-radius limit has to be taken in the end. This limit naturally brings in divergences, which can be usually dealt with, e. g., by the Gibbons–Hawking prescription. The final regularized result is called $I^{R_{\mathrm{BIG}}}_{\mathrm{net}}$ below.

With the notation used above and by setting (because

of the square, the notation below differs from the one used in Ref. [27])

$$A_{\rm M}^2 = 1, \quad A_{\rm S}^2 = 1 - \frac{2GM}{R}, \tag{2}$$

the above terms can be written as [27][1)]

$$I^{\rm wall}_{\rm matter} = -\int_{\tau^{\rm i}}^{\tau^{\rm f}} m(\hat{R})\, d\tau, \tag{3}$$

$$I^{\rm wall}_{\rm gravity} = \int_{\tau^{\rm i}}^{\tau^{\rm f}} d\tau \left\{ \frac{1}{2G} \left[2\hat{R}\epsilon(\hat{R}_{,\tau}^2 + A^2)^{1/2} + \right.\right. \\ \left.\left. + \frac{\hat{R}^2}{\epsilon(\hat{R}_{,\tau}^2 + A^2)^{1/2}} \left(\hat{R}_{,\tau\tau} + \frac{1}{2}(A^2)_{,R} \right) \right] \right\}, \tag{4}$$

$$I^{\rm wall}_{\rm surface} = -\frac{1}{2G} \int_{\tau^{\rm i}}^{\tau^{\rm f}} d\tau \frac{d}{d\tau} \times \\ \times \left[\hat{R}^2 \log\left(\frac{(\hat{R}_{,\tau}^2 + A^2)^{1/2} + \epsilon \hat{R}_{,\tau}}{A} \right) \right] = \\ = -\frac{1}{2G} \int_{\tau^{\rm i}}^{\tau^{\rm f}} d\tau \left[2\hat{R}\hat{R}_{,\tau} \log\left(\frac{(\hat{R}_{,\tau}^2 + A^2)^{1/2} + \epsilon \hat{R}_{,\tau}}{A} \right) + \right. \\ + \frac{\hat{R}^2}{\epsilon(\hat{R}_{,\tau}^2 + A^2)^{1/2}} \left(\hat{R}_{,\tau\tau} + \frac{(A^2)_{,R}}{2} \right) - \\ \left. - \frac{\hat{R}^2 \epsilon(\hat{R}_{,\tau}^2 + A^2)^{1/2}}{2A^2} (A^2)_{,R} \right], \tag{5}$$

$$I^{R_{\rm BIG}}_{\rm surface} = \left(\frac{R_{\rm BIG}}{G} - \frac{3M_\infty}{2} \right) \left(t_{\rm S}^{\rm f} - t_{\rm S}^{\rm i} \right), \tag{6}$$

$$I^{R_{\rm BIG}}_{\rm net} = I^{R_{\rm BIG}}_{\rm surface} - (I_{\rm surface})_0 = \\ = -\frac{M_\infty}{2} \left(t_{\rm S}^{\rm f} - t_{\rm S}^{\rm i} \right) + O\left(\frac{1}{R_{\rm BIG}} \right), \tag{7}$$

where square brackets represent the jump of the bracketed quantities across the shell, i. e.,

$$\left[\hat{B}\right] = \lim_{\delta \to 0^+} \left(\hat{B}(\hat{r} - \delta) - \hat{B}(\hat{r} + \delta) \right). \tag{8}$$

[1)] The expression for $I^{\rm wall}_{\rm surface}$ given in Ref. [27] looks slightly different, but it is equivalent to this one as long as we require that $I^{\rm wall}_{\rm surface}$ be always real valued. As we explain later (see Eq. (19)), the sign flip of ϵ is only important in the Euclidean regime. Because the argument of the logarithm has a jump there, we may have to add one more term proportional to a δ function at the sign flipping point to the right-hand side of Eq. (5). However, the crucial point is that the analyticity of $I^{\rm wall}_{\rm surface}$ is broken at the sign flipping point. Therefore, it is difficult to find a consistent meaning for the analytic continuation of this expression to the Euclidean region.

Square brackets are not used anywhere in this paper with a different meaning. Moreover, the signs

$$\epsilon_\pm = {\rm sign}\left(A_{\rm M}^2 - A_{\rm S}^2 \mp \frac{G^2 m^2}{\hat{R}^2} \right) \tag{9}$$

are unambiguously determined by the consistency with the junction condition [28]

$$\frac{Gm}{\hat{R}} = \left[\epsilon \left(\hat{R}_{,\tau}^2 + A^2 \right)^{1/2} \right]. \tag{10}$$

Noticing that

$$\frac{dt_{\rm S}}{d\tau} = \frac{\epsilon \left(\hat{R}_{,\tau}^2 + A_{\rm S}^2 \right)^{1/2}}{A_{\rm S}^2}, \tag{11}$$

we can combine all the above contributions into the Lagrangian

$$L = \frac{1}{G} \frac{d\tau}{dt_{\rm S}} \left(\left\{ \hat{R} \left[\epsilon (\hat{R}_{,\tau}^2 + A^2)^{1/2} \right] - m(\hat{R}) \right\} - \right. \\ \left. - \hat{R}\hat{R}_{,\tau} \left[\log\left(\frac{(\hat{R}_{,\tau}^2 + A^2)^{1/2} + \epsilon \hat{R}_{,\tau}}{A} \right) \right] \right) - M. \tag{12}$$

Finally, adding a constant M to the Lagrangian such that the Lagrangian vanishes at the turning point, $\hat{R}_{,\tau} = 0$, we can evaluate L on a classical solution to obtain

$$L|_{\rm solution} = -\frac{\hat{R}\hat{R}_{,t_{\rm S}}}{G} \times \\ \times \left[\log\left(\frac{(\hat{R}_{,\tau}^2 + A^2)^{1/2} + \epsilon \hat{R}_{,\tau}}{A} \right) \right]. \tag{13}$$

Here, $\hat{R}_{,\tau}$ is to be replaced with its classical solution, which is obtained from the junction condition (10) as

$$\hat{R}_{,\tau}^2 = \frac{G^2 m^2}{4\hat{R}^2} \left\{ 1 - \frac{(A_{\rm S} + A_{\rm M})^2 \hat{R}^2}{G^2 m^2} \right\} \times \\ \times \left\{ 1 - \frac{(A_{\rm S} - A_{\rm M})^2 \hat{R}^2}{G^2 m^2} \right\}. \tag{14}$$

As explicitly seen above, the action could in general contain second-derivative terms. These second derivatives are removed by the "careful" inclusion of the boundary term, $I^{\rm wall}_{\rm surface}$. From Eq. (13), we identify the effective momentum conjugate to $\hat{R}$ as

$$P_{\rm eff} := -\frac{\hat{R}}{G} \left[\log\left(\frac{(\hat{R}_{,\tau}^2 + A^2)^{1/2} + \epsilon \hat{R}_{,\tau}}{A} \right) \right]. \tag{15}$$

After Wick rotation to Euclidean time, $\bar{\tau} = i\tau$, the Euclidean momentum, $\bar{P}_{\rm eff} = -iP_{\rm eff}$ and Eq. (14) become

$$\bar{P}_{\rm eff} = i\frac{\hat{R}}{G}\left[\log\left(\frac{(A^2 - \hat{R}^2_{,\bar{\tau}})^{1/2} + i\epsilon\hat{R}_{,\bar{\tau}}}{A}\right)\right] \qquad (16)$$

and

$$\hat{R}^2_{,\bar{\tau}} = \frac{G^2m^2}{4\hat{R}^2}\left\{\frac{(A_{\rm S}+A_{\rm M})^2\hat{R}^2}{G^2m^2} - 1\right\} \times \\ \times \left\{1 - \frac{(A_{\rm S}-A_{\rm M})^2\hat{R}^2}{G^2m^2}\right\}. \qquad (17)$$

We indicate quantities after the Wick rotation with "$-$", if they are different from the Lorentzian ones. We also note that $\bar{P}_{\rm eff}$ is real, since the modulus of the argument inside the logarithm is unity. Then the tunnelling action can be evaluated as

$$\bar{I}_{(t_{\rm S})} = \int d\bar{t}_{\rm S}\hat{R}_{,t_{\rm S}}\bar{P}_{\rm eff} \qquad (18)$$

to provide the tunnelling rate proportional to $\exp(-2\bar{I}_{(t_{\rm S})})$.

3. WORMHOLE PRODUCTION

The framework discussed in the preceding section is generically applicable to the tunnelling problem. However, analytic continuation brings up situations that are technically and conceptually more involved. To see this, we first notice that $\epsilon = \pm 1$ flips sign when

$$A^2_{\pm} + \hat{R}^2_{,\tau} = \frac{G^2m^2}{4\hat{R}^2}\left(1 \pm \frac{(A^2_{\rm S} - A^2_{\rm M})\hat{R}^2}{G^2m^2}\right)^2 = \\ = \frac{G^2m^2}{4\hat{R}^2}\left(1 \mp \frac{R_{\rm g}\hat{R}}{G^2m^2}\right)^2 \qquad (19)$$

vanishes, where $R_{\rm g} := 2GM$. We denote by $\hat{R}_{\rm c}$ the value of $\hat{R}$ at the sign changing point. In the Lorentzian regime, the sign flip of ϵ does not occur in regions outside horizons: it can happen behind horizons, but in these cases no pathology arises [26]. In any case, in this work, because of our definitions (2), we implicitly exclude regions behind horizons. This is certainly nonrestrictive for our current purpose, because it is possible to prove that tunnelling *must always begin and end* in regions that are *not* behind the horizons, and it is always true that $P_{\rm eff}$ is continuous during the time evolution. However, in the Euclidean regime, not only the sign flip can happen, but also the argument of the logarithm (and hence the logarithm itself) in $P_{\rm eff}$ has a jump at the point where the sign of ϵ flips: this cannot be avoided if we consistently require that the effective momentum vanishes at both turning points. (In fact, the discontinuity cannot be avoided if we require that $P_{\rm eff}$ analytically continued back to the Lorentzian regime be real both before and after the tunnelling.) This happens because the expression for $P_{\rm eff}$ is essentially nonanalytic. For this reason, it is hard to justify the use of analytic continuation for an action that contains $P_{\rm eff}$.

In the present case, from Eq. (19), we find that the sign flip can happen for ϵ_+ only. From the analytic continuation of Eq. (11),

$$\frac{d\bar{t}_{\rm S}}{d\bar{\tau}} = \frac{\epsilon\left(A^2_{\rm S} - \hat{R}^2_{,\bar{\tau}}\right)^{1/2}}{A^2_{\rm S}}, \qquad (20)$$

we find that $d\bar{t}_{\rm S}/d\bar{\tau}$ also vanishes at the sign flip point. This means that the trajectory of the wall becomes purely radial. At this point, there is a jump of the logarithm in $\bar{P}_{\rm eff}$. We draw a schematic picture of the wall trajectory when there is a sign flip in Fig. 1. In this picture, the center corresponds to $R = 2GM$, the radial direction is the rescaled radius, and the angular direction is the Euclidean time $\bar{t}_{\rm S}$.

As a concrete example, we consider the case of a pure tension wall with $m = 4\pi\sigma R^2$. In this case, from Eq. (14), we find that the turning points corresponding to $\hat{R}_{,\tau} = 0$ are given by the solutions of

$$f(\hat{R}) := \tilde{\sigma}^2\hat{R}^3 - 2\tilde{\sigma}\hat{R}^2 + R_{\rm g} = 0, \qquad (21)$$

where we set $\tilde{\sigma} := 4\pi G\sigma$. It is easy to see that $f(R_{\rm g}) \geq \\ \geq 0$ and the equality holds for $\tilde{\sigma} = 1/R_{\rm g}$. At the minimum of $f(\hat{R})$, where $\hat{R} = 4/3\tilde{\sigma}$, we have $f(4/3\tilde{\sigma}) = \\ = R_{\rm g} - 32/27\tilde{\sigma}$. Therefore, we find that there is a classically forbidden region for $\tilde{\sigma} < 32/27R_{\rm g}$. A wormhole can be produced when the critical radius, where the discontinuity appears,

$$\hat{R}_{\rm c} = \left(\frac{R_{\rm g}}{\tilde{\sigma}^2}\right)^{1/3}, \qquad (22)$$

is in the classically forbidden region. As mentioned above, this critical radius does not result in pathologies in the classically allowed region. Therefore, if $\hat{R}_{\rm c} > R_{\rm g}$, the critical radius is under the potential barrier. This means that wormhole production is possible when $\tilde{\sigma} < \\ < 1/R_{\rm g}$.

Now, we discuss the key issue of this paper. As long as we use the foliation by the Schwarzschild time,

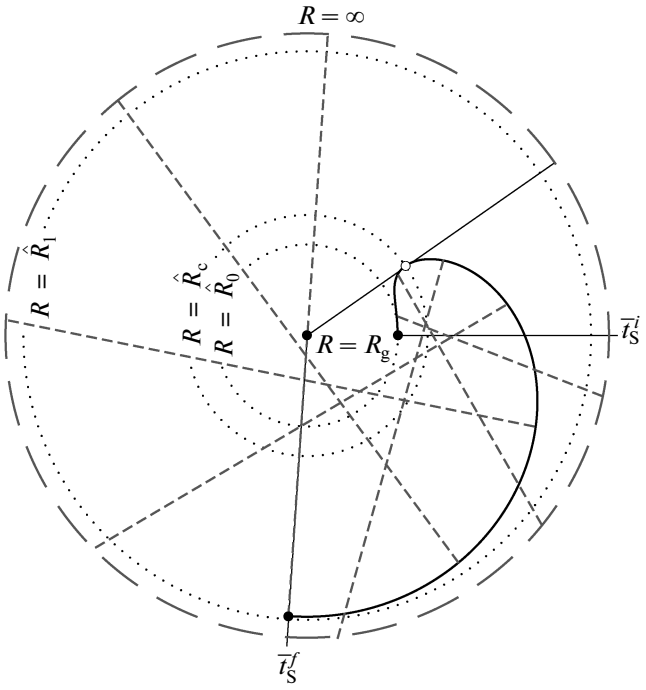

Fig. 1. A schematic diagram of the Euclidean Schwarzschild spacetime. The center and the boundary of the circle respectively correspond to $R = R_g$ and $R = \infty$. Dotted circles show the surface $R = \hat{R}_c$ and those corresponding to the radii of the turning points, $R = \hat{R}_{0,1}$. The angle represents the direction of the time coordinate of the static chart, $\bar{t}_S$. The solid curve represents the trajectory of the domain wall, for the Minkowski–Schwarzschild case with $M = 1$ and $\tilde{\sigma} = 0.25$. Surfaces with $\bar{t}_S = \text{const}$ are shown by solid lines. The foliation by these surfaces starts with $\bar{t}_S = \bar{t}_S^i$ and the angle increases at the beginning. After reaching the maximum, the angle starts to decrease to reach $\bar{t}_S = \bar{t}_S^f$. The foliation corresponding to a smooth time slicing is presented by dashed lines

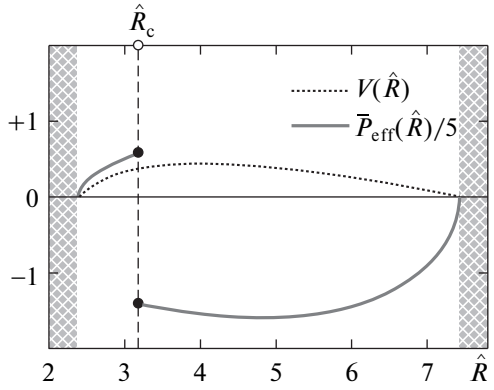

Fig. 2. Plot of the effective potential and of the effective Euclidean momentum along a tunnelling trajectory. The quantities are calculated for a Minkowski–Schwarzschild junction in which $M = 1$ and $\tilde{\sigma} = 0.25$, which results in the relevant sign for the outside spacetime to change at $\hat{R}_c \approx 3.175$. The plot clearly emphasizes the discontinuity in the expression for the effective momentum (16) due to the change in the ϵ_+ sign

it is problematic to consistently define the Euclidean manifold interpolating between the configurations before and after the tunnelling. As a concrete example, we consider the case shown in Fig. 1 (for this case, plots of the effective momentum along the tunnelling trajectory and of the potential barrier can be found in Fig. 2). When $d\bar{t}_S/d\bar{\tau}$ is positive, the wall is located at $\hat{R} < \hat{R}_c$ and the Schwarzschild spacetime is relevant for $\hat{R} < R < \infty$. The Minkowski spacetime is connected beyond the wall. After passing through the point $\hat{R} = \hat{R}_c$, $d\bar{t}_S/d\bar{\tau}$ becomes negative. Then, the wall is present for $\hat{R} > \hat{R}_c$ and the Schwarzschild spacetime is relevant for $R < \hat{R}$. Again, the Minkowski spacetime is connected beyond the wall. Then, one may wonder where the asymptotic region with $R \to \infty$ is. The asymptotic region is on the other side extending beyond the center, corresponding to $R = 2GM$. The time slice cannot terminate at the center (bifurcation point) of the Schwarzschild spacetime. We then see that the geometry on this time slice suddenly changes at the sign flip point. Namely, the final configuration contains a wormhole, corresponding to the existence of a minimum circumferential radius. At the same time, $\bar{P}_{\text{eff}}$ is discontinuous there. As long as we stick to this time slice, it is difficult to obtain a satisfactory and consistent prescription. Figures 3 and 4 show the situation before and after the tunnelling. By comparing the slice before the tunnelling (thick horizontal line in the Penrose diagram for the configuration before the tunnelling in Fig. 3*c*) with the slice after the tunnelling (thick horizontal line in the Penrose diagram for the configuration after the tunnelling in Fig. 4*c*), we can also have a clear example of the situation discussed just above for the Euclidean spacetime that should interpolate between these two configurations. In the next section, we discuss the same process in the canonical formalism without specifying the gauge, which makes it possible to overcome these difficulties.

4. CANONICAL APPROACH WITH SMOOTH TIME SLICE

We consider the canonical approach in this section, following Ref. [29]. The spherically symmetric metric

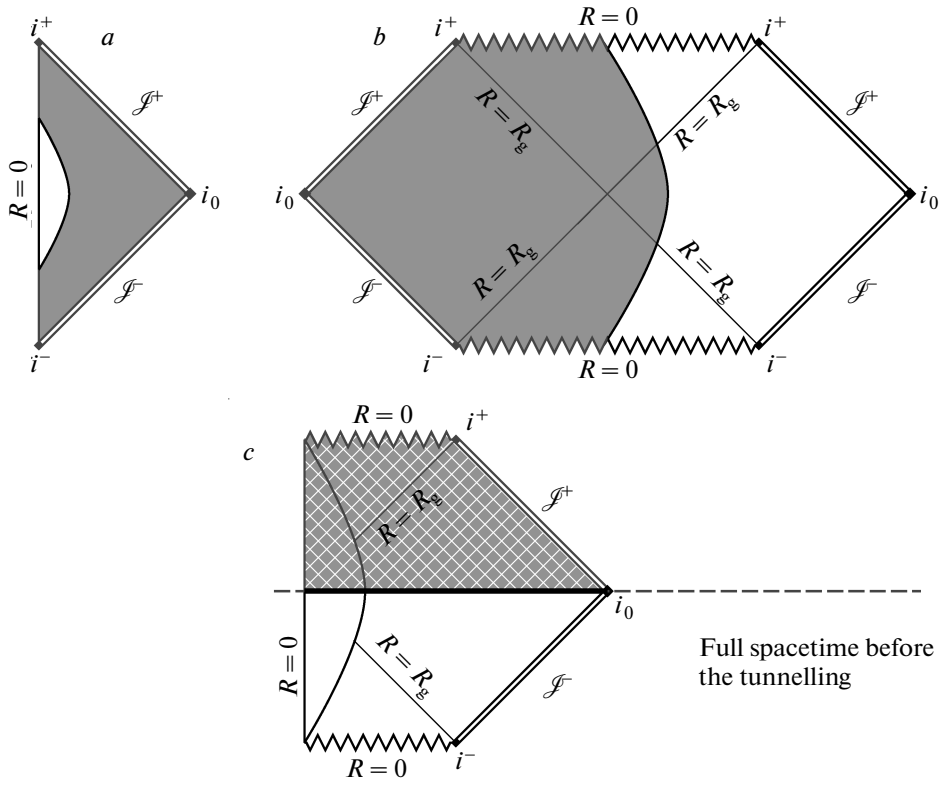

Fig. 3. Construction of the Penrose diagram for the spacetime before the tunnelling. Panel a shows the wall trajectory in Minkowski spacetime. The unshaded area between $R=0$ and the bubble wall participates in the junction and is joined to the unshaded region of the Schwarzschild spacetime in panel b. The final configuration is shown in panel c, where, again, we have to consider only the unshaded part of the Penrose diagrams, that describes spacetime while the wall expands from $R=0$ until the turning point, where tunnelling takes place. The thick black line in panel c is the spacetime slice at which tunnelling starts (see, e. g., the $\bar{t}^{\,\mathrm{i}}_{\mathrm{S}}$ slice in Fig. 1, which corresponds to the Schwarzschild part of this slice)

is specified in the $3+1$ decomposition as

$$ds^2 = N^t dt^2 + L^2(dr + N^r dt)^2 + R^2 d\Omega^2, \qquad (23)$$

where, with the standard notation, $d\Omega^2$ is the spherically symmetric part of the line element. Then the action in the canonical formalism is obtained as

$$S = \int dt\, p\,\dot{\hat{r}} + \int dt \int dr \times$$
$$\times \left(\frac{1}{G}\{\pi_L \dot{L} + \pi_R \dot{R}\} - N^t \mathcal{H}_t - N^r \mathcal{H}_r\right) - \int dt_{\mathrm{S}} M \qquad (24)$$

with

$$\mathcal{H}_t = \frac{1}{G}\left(\frac{L\pi_L^2}{2R^2} - \frac{\pi_L \pi_R}{R} + \left(\frac{RR'}{2L}\right)' - \frac{R'^2}{2L} - \frac{L}{2}\right) +$$
$$+ \delta(r-\hat{r})\sqrt{\left(\frac{p}{\hat{L}}\right)^2 + m^2}, \qquad (25)$$

$$\mathcal{H}_r = \frac{1}{G}\left(R'\pi_R - L\pi_L'\right) - \delta(r-\hat{r})\, p,$$

where p, π_L, and π_R are the respective conjugate momenta to $\hat{r}$, L, and R. For the derivatives, we adopt the following standard convention:

$$\dot{B} = \frac{\partial B}{\partial t}, \quad B' = \frac{\partial B}{\partial r}. \qquad (26)$$

We stress that the values of all the metric functions are assumed to be continuous across the wall, although their derivatives can be discontinuous. The constraint equations $\mathcal{H}_t = 0$ and $\mathcal{H}_r = 0$ are solved in the bulk as

$$\pi_L = R\beta, \quad \pi_R = \frac{\pi_L'}{X}, \qquad (27)$$

where we introduce the definitions

$$X := \frac{R'}{L}, \quad \beta := (X^2 - A^2)^{1/2}. \qquad (28)$$

By integrating the constraint equations across the wall, we obtain the junction conditions, which in the present notation can be written as

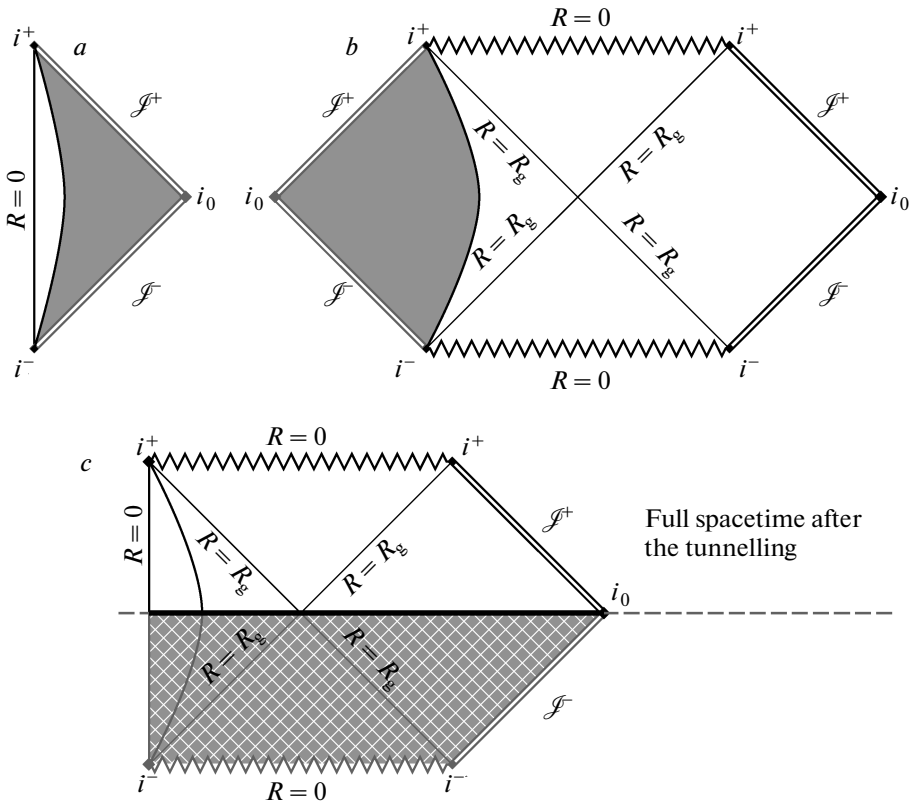

Fig. 4. Construction analogous to the one in Fig. 3, but for the spacetime after the tunnelling. The junction is obtained again by joining the unshaded region of the Minkowski spacetime in panel *a*, with the unshaded region of the Schwarzschild spacetime in panel *b*. After performing the junction, the spacetime after the tunnelling is the region to the future of the thick black line in panel *c*. The part of this slice in the Schwarzschild region corresponds to the $\bar{t}_{\rm S}^{\rm f}$ slice in Fig. 1. Here it is also clear that after the tunnelling, the slice contains $R = R_g$. This was not the case for the slice before the tunnelling shown in Fig. 3

$$[\pi_L] = \frac{Gp}{\hat{L}}, \quad [X] = \frac{Gm}{\hat{R}}\left(1 + \frac{p^2}{m^2\hat{L}^2}\right)^{1/2}. \tag{29}$$

In the WKB approximation, the wave function is written as $\propto \exp(iI(\hat{r}, L, R))$ and the conjugate momenta are identified as

$$p = \frac{\delta I}{\delta \hat{r}}, \quad \pi_L = G\frac{\delta I}{\delta L}, \quad \pi_R = G\frac{\delta I}{\delta R}. \tag{30}$$

Hence, the action relevant to the WKB wave function is

$$I = \int dt\, p\dot{\hat{r}} + \frac{1}{G}\left(\int dt \int dr\{\pi_L \dot{L} + \pi_R \dot{R}\}\right). \tag{31}$$

We note that in this approach, removing the last term in Eq. (24) is absolutely unambiguous.

To handle expression (31) without specifying the gauge, a key observation is the existence of a function $\Phi = \Phi(L, R, R')$ that satisfies

$$\delta\Phi \sim \pi_L \delta L + \pi_R \delta R, \tag{32}$$

where "$\sim$" means that the equality holds modulo total derivative terms. It is then possible to integrate the above equation to obtain

$$\Phi(L, R, R') = RR' \log\left(\frac{X - \beta}{A}\right) + RL\beta. \tag{33}$$

In the above expression, there is an arbitrariness because the total derivative of an arbitrary function of R with respect to r can be added, which, of course, does not affect the final result.

Then the action becomes

$$I = \int dt\, p\dot{\hat{r}} + \frac{1}{G}\left(\int dr \int dt \frac{\partial\Phi}{\partial t} - \int dt\left[\Psi\dot{R}\right]\right) =$$
$$= \int dt\, p\dot{\hat{r}} + \frac{1}{G} \times$$
$$\times \left(\int dr\, \Phi\Big|_{t_{\rm S}^{\rm i}}^{t_{\rm S}^{\rm f}} - \int dt\, \dot{\hat{r}}[\Phi] - \int dt\left[\Psi\dot{R}\right]\right), \tag{34}$$

where we define

$$\Psi := \frac{\partial \Phi}{\partial R'} = R \log\left(\frac{X-\beta}{A}\right). \tag{35}$$

In the first equality in Eq. (34), we removed the contribution of $\Psi\dot{R}$ at $r \to \infty$, assuming that the time slice is asymptotically identical to the one in the static chart of the Schwarzschild spacetime, in which Ψ vanishes because $\beta = 0$ and $X = A$. Using

$$\dot{\hat{R}} := \frac{d\hat{R}}{dt} = \left(R'\dot{\hat{r}} + \dot{R}\right)_{r=\hat{r}}, \tag{36}$$

we can rewrite the last term in the parentheses in the right-hand side of Eq. (34) as

$$\left[\Psi\dot{R}\right] = \left[\Psi\dot{\hat{R}} - \Psi R'\dot{\hat{r}}\right] = -\left[\Psi R'\right]\dot{\hat{r}} + \left[\Psi\right]\dot{\hat{R}}, \tag{37}$$

where in the last equality we have extracted $\dot{\hat{R}}$ and $\dot{\hat{r}}$ from the square brackets since their values evaluated on both sides of the junction are identical. Thus, we obtain

$$I = \int dt\,\dot{\hat{r}}\left(p + \frac{1}{G}\left[\Psi R' - \Phi\right]\right) + \\ + \frac{1}{G}\left(\int dr\,\Phi\Big|_{t_{\rm S}^{\rm i}}^{t_{\rm S}^{\rm f}} - \int dt\,\dot{\hat{R}}\left[\Psi\right]\right). \tag{38}$$

Because we have $\Psi R' - \Phi = -RL\beta$, the first term in Eq. (38) vanishes under the junction condition (29), and we finally obtain the *gauge nonfixed* action relevant for the WKB wave function in the form

$$I = \frac{1}{G}\left(\int dr\,\Phi\Big|_{t_{\rm S}^{\rm i}}^{t_{\rm S}^{\rm f}} - \int dt\,\dot{\hat{R}}\left[\Psi\right]\right). \tag{39}$$

We now examine the motion of the shell, $d\hat{R}/dt$, in more detail. The part of the action related to the shell takes the form

$$S_{\rm s} = \int dt\,L_{\rm s} = \\ = -m\int dt\left((\hat{N}^t)^2 - \hat{L}^2(\dot{\hat{r}} + \hat{N}^r)^2\right)^{1/2}. \tag{40}$$

From this expression, the conjugate momentum to $\hat{r}$ turns out to be given by

$$p = \frac{\partial L_{\rm s}}{\partial \dot{\hat{r}}} = \\ = m\left((\hat{N}^t)^2 - \hat{L}^2(\dot{\hat{r}} + \hat{N}^r)^2\right)^{-1/2}\hat{L}^2(\dot{\hat{r}} + \hat{N}^r), \tag{41}$$

from which we obtain

$$\frac{\hat{L}^2}{(\hat{N}^t)^2}(\dot{\hat{r}} + \hat{N}^r)^2 = \frac{p^2}{m^2\hat{L}^2}\left(1 + \frac{p^2}{m^2\hat{L}^2}\right)^{-1}. \tag{42}$$

From the normalization of the four velocity, we also find

$$\left(\frac{\hat{N}^t d\hat{t}}{d\tau}\right)^2\left(1 - \frac{\hat{L}^2}{(\hat{N}^t)^2}(\dot{\hat{r}} + \hat{N}^r)^2\right) = 1, \tag{43}$$

which is further simplified using Eq. (42) as

$$\frac{\hat{N}^t d\hat{t}}{d\tau} = \left(1 + \frac{p^2}{m^2\hat{L}^2}\right)^{1/2}. \tag{44}$$

Now, we are ready to rewrite $d\hat{R}/d\tau$. Using the equation of motion for R, we have

$$\dot{R} = -N^t\frac{\pi_L}{R} + N^r R'.$$

Then we obtain

$$\frac{d\hat{R}}{d\tau} = \frac{d\hat{t}}{d\tau}\left((\hat{N}^r + \dot{\hat{r}})\hat{R}' - \hat{N}^t\frac{\hat{\pi_L}}{\hat{R}}\right) = \\ = \frac{\hat{N}^t d\hat{t}}{d\tau}\left((\hat{N}^r + \dot{\hat{r}})\frac{\hat{L}}{\hat{N}^t}\hat{X} - \hat{\beta}\right) = \\ = \left(1+\frac{p^2}{m^2\hat{L}^2}\right)^{1/2}\left(\left(1+\frac{p^2}{m^2\hat{L}^2}\right)^{-1/2}\frac{p\hat{X}}{m\hat{L}} - \hat{\beta}\right) = \\ = \frac{p\hat{X}}{m\hat{L}} - \hat{\beta}\left(1 + \frac{p^2}{m^2\hat{L}^2}\right)^{1/2}, \tag{45}$$

where in the third equality, we have used Eqs. (42) and (44). Substituting $\hat{\beta} = (\hat{X}^2 - \hat{A}^2)^{1/2}$, we can solve this equation for $\hat{X}$ as

$$\hat{X} = -\frac{p}{m\hat{L}}\hat{R}_{,\tau} + \epsilon\left(\hat{R}_{,\tau}^2 + \hat{A}^2\right)^{1/2}\left(1+\frac{p^2}{m^2\hat{L}^2}\right)^{1/2}. \tag{46}$$

Remembering that p and $\hat{R}_{,\tau}$ do not have a jump across the junction, from Eq. (46) and the junction condition (29), we recover exactly Eq. (10).

Furthermore, substituting Eq. (46) in Eq. (45), we obtain

$$\hat{\beta} = -\left(1+\frac{p^2}{m^2\hat{L}^2}\right)^{1/2}\hat{R}_{,\tau} + \epsilon\frac{p}{m\hat{L}}\left(\hat{R}_{,\tau}^2 + \hat{A}^2\right)^{1/2}, \tag{47}$$

and hence

$$\hat{X} - \hat{\beta} = \left\{\left(1 + \frac{p^2}{m^2\hat{L}^2}\right)^{1/2} - \frac{p}{m\hat{L}}\right\} \times \\ \times\left\{\epsilon\left(\hat{R}_{,\tau}^2 + \hat{A}^2\right)^{1/2} + \hat{R}_{,\tau}\right\}. \tag{48}$$

Therefore, we can finally write the jump of Ψ as

$$\left[\Psi\right] = \hat{R}\left[\log\left(\frac{\epsilon\left(\hat{R}_{,\tau}^2 + A^2\right)^{1/2} + \hat{R}_{,\tau}}{A}\right)\right]. \tag{49}$$

After Euclideanization, Eq. (39) can be rewritten using the above results, and it gives

$$\bar{I} = \frac{1}{G}\left(\int dr\,\bar{\Phi}\Big|_{\bar{t}^{\,\mathrm{i}}_{\mathrm{S}}}^{\bar{t}^{\,\mathrm{f}}_{\mathrm{S}}} - \int dt\,\dot{\hat{R}}[\bar{\Psi}]\right) \tag{50}$$

with

$$\bar{\Phi} = i\Phi = iRR'\log\left(\frac{X - i\left(A^2 - X^2\right)^{1/2}}{A}\right) - \\ - RL\left(A^2 - X^2\right)^{1/2} \tag{51}$$

and

$$[\bar{\Psi}] = [i\Psi] = i\hat{R}\left[\log\left(\frac{\epsilon\left(A^2 - \hat{R}^2_{,\bar{\tau}}\right)^{1/2} + i\hat{R}_{,\tau}}{A}\right)\right]. \tag{52}$$

This expression is identical to Eq. (18) obtained in Sec. 2 for the tunnelling that does not produce a wormhole. First, since $A = X$ on the initial and final surfaces, where the time slices coincide with the ones with $\bar{t}_{\mathrm{S}} = \mathrm{const}$ and $\bar{t}_{\mathrm{M}} = \mathrm{const}$, $\bar{\Phi}$ vanishes there. Since $\epsilon = +1$ in this case, as mentioned above, the difference between $\bar{P}_{\mathrm{eff}}$ and $[\bar{\Psi}]$ does not arise.

By contrast, in the case with wormhole production, the first term in Eq. (50) does not vanish because X is negative in the region between $R = R_{\mathrm{g}}$ and the wall in the Schwarzschild spacetime, and hence $X = -A$ there. Namely, the first term contributes as

$$\int dr\,\bar{\Phi}\Big|_{\bar{t}^{\,\mathrm{i}}_{\mathrm{S}}}^{\bar{t}^{\,\mathrm{f}}_{\mathrm{S}}} = \int_{\hat{r}(\bar{t}^{\,\mathrm{f}}_{\mathrm{S}})}^{r_{\mathrm{g}}} dr\,\pi RR' = \frac{1}{2}\left(R_{\mathrm{g}}^2 - \hat{R}(\bar{\tau}^{\mathrm{f}})^2\right), \tag{53}$$

where r_{g} is the value of r at $R = R_{\mathrm{g}}$ on the final surface. Hence, the difference between Eqs. (18) and (50) is evaluated as

$$\bar{I} - \bar{I}_{(t_{\mathrm{S}})} = \int dr\,\bar{\Phi}\Big|_{\bar{t}^{\,\mathrm{i}}_{\mathrm{S}}}^{\bar{t}^{\,\mathrm{f}}_{\mathrm{S}}} + \\ + \pi\int_{R_c}^{\hat{R}(\bar{t}^{\,\mathrm{i}}_{\mathrm{S}})} dR\,R = \frac{1}{2}\left(R_{\mathrm{g}}^2 - R_c^2\right), \tag{54}$$

if we assume that $\bar{P}_{\mathrm{eff}}$ in Eq. (18) has a discrete jump at $\hat{R} = R_{\mathrm{c}}$. Of course, this discrepancy is not strange at all, since the naive extension of the validity range of formula (18) cannot be justified.

5. CONSISTENT DIRECT EVALUATION

As we anticipated, we now show that the method using a *pseudo-manifold* for the description of the instanton solution gives the same result that we derived using the canonical approach in the preceding section. Although this equivalence might seem almost trivial because both approaches are based on the same smooth foliation of an Euclidean spacetime, its explicit proof would be pedagogically useful.

We then return to the discussion in Sec. 2. The first key observation is that the contribution from the carefully included $I^{\mathrm{wall}}_{\mathrm{surface}}$ should not be included when we adopt a smooth foliation. The second point is that we have rewritten a term in Eq. (4) as

$$\int_{\tau^{\mathrm{i}}}^{\tau^{\mathrm{f}}} d\tau\frac{\hat{R}^2(\hat{A}_{\mathrm{S}})^2_{,\hat{R}}}{4G\epsilon(\hat{R}^2_{,\tau} + A^2)^{1/2}} = -\frac{M}{2}\int_{\tau^{\mathrm{i}}}^{\tau^{\mathrm{f}}} d\tau\frac{d\hat{t_{\mathrm{S}}}}{d\tau}. \tag{55}$$

We then subtracted $M(t^{\mathrm{f}}_{\mathrm{S}} - t^{\mathrm{i}}_{\mathrm{S}})$ from the total action. In the computation in Sec. 2, half of this subtraction was compensated by $I^{R_{\mathrm{BIG}}}_{\mathrm{surface}}$ and the rest by the above contribution (55). However, we find

$$\int_{\bar{\tau}^{\mathrm{i}}}^{\bar{\tau}^{\mathrm{f}}} d\bar{\tau}\frac{d\hat{t}_{\mathrm{S}}}{d\bar{\tau}} = \bar{t}^{\,\mathrm{f}}_{\mathrm{S}} - \bar{t}^{\,\mathrm{i}}_{\mathrm{S}} + 2\pi R_{\mathrm{g}}, \tag{56}$$

when we use a smooth foliation for the tunnelling solution with wormhole formation. This shows that an additional contribution $\pi M R_{\mathrm{g}}$ to the Euclidean action arises. Gathering all, we find that the Euclidean action evaluated by using a smooth foliation is given by

$$\bar{I}_{(t_{\mathrm{S}})} - \bar{I}^{\mathrm{wall}}_{\mathrm{surface}} + \pi M R_{\mathrm{g}} = \\ = \frac{1}{G}\left(-\int dt\,\dot{\hat{R}}\,[\bar{\Psi}] + \frac{\hat{R}}{2}\hat{\bar{\Phi}}\Big|_{\bar{t}^{\,\mathrm{i}}_{\mathrm{S}}}^{\bar{t}^{\,\mathrm{f}}_{\mathrm{S}}} + \frac{R_{\mathrm{g}}^2}{2}\right) = \\ = \frac{1}{G}\left(-\int dt\,\dot{\hat{R}}\,[\bar{\Psi}] + \frac{R_{\mathrm{g}}^2 - \hat{R}(\bar{\tau}^{\mathrm{f}})}{2}\right), \tag{57}$$

which is precisely identical to $\bar{I}$.

6. SUMMARY AND DISCUSSION

In this paper, we studied the wormhole production for the simplest spherically symmetric shell model in asymptotically flat spacetime. In this simple setup, the instanton solution can be generically described by the junction of Euclideanized Minkowski and Schwarzschild spacetimes. This solution, however, is not a Riemannian manifold in the sense that the existence of the domain wall may depend on the path taken to reach the possible location of the wall in spacetime. The term *pseudo-manifold* was used in [27] for this solution. A key point that we have emphasized here is that in this case, the ordinary constant-time surfaces associated with the static chart do not foliate the instanton

smoothly. As a result, methods based on this time slicing inevitably become conceptually ambiguous.

We have here discussed, however, that even in these cases, if we choose a smooth time slicing to connect the configurations before and after the tunnelling, it is still possible to find the WKB wave function along an interpolating path of configurations with a bubble wall. In this way, we can identify an appropriate expression for the tunnelling rate without any ambiguity. The result agrees with the direct evaluation of the Euclidean action once we properly subtract the zero-point energy and count how many times each region in the instanton solution is swept when we consider a smooth foliation.

It is possible to trace the subtle nature of the *pseudo-manifold* to the fact that the time lapse in the Euclidean region is not positive everywhere. Indeed, the sign of the time lapse has to be opposite between the center and the asymptotic infinity, for at least some range during the time evolution. This is a feature that is common to the upward tunnelling in the case of bubble nucleation. It would be worth investigating whether this negative lapse causes any problem when we take fluctuations around the WKB trajectory into account.

This work was supported in part by the Grant-in-Aid for Scientific Research (Nos. 24103006, 24103001, and 26287044). One of us, S. A., would like to heartfully thank the Department of Physics of Kyoto University for extended hospitality and support.

REFERENCES

1. S. R. Coleman, Phys. Rev. D **15**, 2929 (1977) [Erratum — ibid. D **16**, 1248 (1977)].
2. C. G. Callan Jr. and S. Coleman, Phys. Rev. D **16**, 1762 (1977).
3. S. R. Coleman and F. De Luccia, Phys. Rev. D **21**, 3305 (1980).
4. J. Garriga, D. Schwartz-Perlov, A. Vilenkin, and S. Winitzki, JCAP **0601**, 017 (2006) [arXiv:hep-th/0509184].
5. S. M. Carroll, M. C. Johnson, and L. Randall, JHEP **0911**, 094 (2009) [arXiv:0904.3115 [hep-th]].
6. J. J. Blanco-Pillado, D. Schwartz-Perlov, and A. Vilenkin, JCAP **1005**, 005 (2010) [arXiv:0912.4082 [hep-th]].
7. J. R. Gott, Nature **295**, 304 (1982).
8. K. Yamamoto, M. Sasaki, and T. Tanaka, Astrophys. J. **455**, 412 (1995) [atXiv:astro-ph/9501109].
9. M. Bucher, A. S. Goldhaber, and N. Turok, Nucl. Phys. Proc. Suppl. **43**, 173 (1995) [arXiv:hep-ph/9501396].
10. M. Bucher and N. Turok, Phys. Rev. D **52**, 5538 (1995) [arXiv:hep-ph/9503393].
11. K.-M. Lee and E. J. Weinberg, Phys. Rev. D **36**, 1088 (1987).
12. J. Garriga and A. Vilenkin, Phys. Rev. D **57**, 2230 (1998) [arXiv:astro-ph/9707292].
13. G. V. Lavrelashvili, V. A. Rubakov, and P. G. Tinyakov, Phys. Lett. B **161**, 280 (1985).
14. T. Tanaka and M. Sasaki, Progr. Theor. Phys. **88**, 503 (1992).
15. T. Tanaka and M. Sasaki, Phys. Rev. D **50**, 6444 (1994) [arXiv:gr-qc/9406020].
16. K. Sato, M. Sasaki, H. Kodama, and K. Maeda, Progr. Theor. Phys. **65**, 1443 (1981).
17. H. Kodama, M. Sasaki, K. Sato, and K. Maeda, Progr. Theor. Phys. **66**, 2052 (1981).
18. K. Sato, Progr. Theor. Phys. **66**, 2287 (1981).
19. K. Maeda, K. Sato, M. Sasaki, and H. Kodama, Phys. Lett. B **108**, 98 (1982).
20. K. Sato, H. Kodama, M. Sasaki, and K. Maeda, Phys. Lett. B **108**, 103 (1982).
21. H. Kodama, M. Sasaki, and K. Sato, Progr. Theor. Phys. **68** 1979 (1982).
22. S. K. Blau, E. I. Guendelman, and A. H. Guth, Phys. Rev. D **35**, 1747 (1987).
23. V. A. Berezin, V. A. Kuzmin, and I. I. Tkachev, Phys. Rev. D **36**, 2919 (1987).
24. V. A. Berezin, V. A. Kuzmin, and I. I. Tkachev, Phys. Rev. D **43**, R3112 (1991).
25. S. Ansoldi and E. I. Guendelman, Progr. Theor. Phys. **120**, 985 (2008).
26. S. Ansoldi, In *Proc. of "From Quantum to Emergent Gravity: Theory and Phenomenology"*, June 11–15, 2007, Trieste, Italy [http://pos.sissa.it/archive/conferences/043/004/QG-Ph_004.pdf].
27. E. Farhi, A. H. Guth, and J. Guven, Nucl. Phys. B **339**, 417 (1990).
28. W. Israel, Nuovo Cim. B **44**, 1 (1966); errata — ibid B **48**, 463 (1967).
29. P. Kraus and F. Wilczek, Nucl. Phys. B **433**, 403 (1995) [arXiv:gr-qc/9408003].